IEEE Access
Multidisciplinary ⋮ Rapid Review ⋮ Open Access Journal

Received May 22, 2020, accepted June 19, 2020, date of publication June 26, 2020, date of current version July 17, 2020.

*Digital Object Identifier 10.1109/ACCESS.2020.3005343*

# Dam Structure Deformation Monitoring by GB-InSAR Approach

**ZHIWEI QIU[1,2], MINGLIAN JIAO[1], TINCHEN JIANG[1], AND LI ZHOU[1]**
[1]School of Marine Technology and Geomatics, Jiangsu Ocean University, Lianyungang 222005, China
[2]State Key Laboratory of Hydrology-Water Resources and Hydraulic Engineering, Nanjing Hydraulic Research Institute, Nanjing 210089, China

Corresponding author: Zhiwei Qiu (qiuzhiwei-2008@163.com)

This work was supported in part by the Scientific Research Project of Surveying and Mapping Geographic Information in Jiangsu Province under Grant JSCHKY201904, in part by the the Belt and Road Special Foundation of the State Key Laboratory of Hydrology-Water Resources and Hydraulic Engineering under Grant 2018491411, in part by the Marine Technology Brand Major of Jiangsu Province under Grant PPZY2015B116, and in part by the Priority Academic Program Development of Jiangsu Higher Education Institutions (PAPD).

**ABSTRACT** Ground-based synthetic aperture radar (GB-SAR) has been proved to be one of the cutting-edge techniques for the timely detection of slope failures in both natural and engineered slopes. This paper focuses on the structure deformation monitoring on the dams using GB-SAR data. Temporal sequence data was collected by ground SAR equipment from 29 July to 1 August for the Geheyan dam and the SAR images with high quality were selected through the exhaustive spatial-temporal coherence analysis based on permanent scatterer (PS) theory in this paper. A practical solution for dam structure deformation extraction after the atmospheric effect reduction is proposed in depth. The deformation of the dam spillway gates is greater than that of the dam body monitored by this GB-SAR campaign, and with the increase of the water level in the reservoir area, the displacement increases along the direction of water flow gradually. The surface deformation rate of the dam body is fitted by linear regression analysis, and the interpolated rate results are compared and verified with the plumb line measurements. Finally, the consistency of the dam deformation average rate based on the PS time series analysis technology by GB-SAR and plumb lines is verified in this article, demonstrated the excellent performance of the proposed method for remote multipoint displacement measurements of the dam.

**INDEX TERMS** GB-SAR, deformation monitoring, permanent scatterer, dam structure, time series analysis.

## I. INTRODUCTION

The image data of the monitoring scope can be obtained using GB-SAR technology, which can actively detect images with microwave. A high spatial resolution radar image in the azimuth and range can be acquired based on the synthetic aperture and step frequency continuous wave (SF-CW) technologies. Sub millimetre micro-deformation can be detected along the line-of-sight (LOS) direction of the radar through interferometric synthetic radar (InSAR) technology [1]. Typical application fields include deformation monitoring of landslide, glacier, dam, building, bridge [2], [3], disaster assessment of earthquake and volcanic activity, and ground subsidence monitoring [4]. GBInSAR is an advanced high-precision, low-cost and continuous monitoring technology. This method can autonomously set sampling frequency and achieve real-time monitoring of the deformation area. GB-SAR has higher spatial-temporal resolution and coherence than spaceborne SAR.

The method for extracting point targets with high coherence was proposed for the PS concept on the basis of time series analysis. Sequential SAR images are analysed in depth by discrete points selected with high phase and amplitude stability. then the phases characteristics of these discrete points are employed to calculate time series deformation. Deformation monitoring technology has been matured and widely applied in spaceborne SAR technique by now. Analysis methods based on PS mainly include PS, IPTA, short baseline set and coherent target methods [5]. The conventional InSAR data processing method cannot be directly applied to GB-SAR monitoring because the monitoring principle is not entirely suitable for the GB-SAR issue. This article aims to propose a practical methodology based on PS points analysis to obtain the dam structure deformation

The associate editor coordinating the review of this manuscript and approving it for publication was Jenny Mahoney.

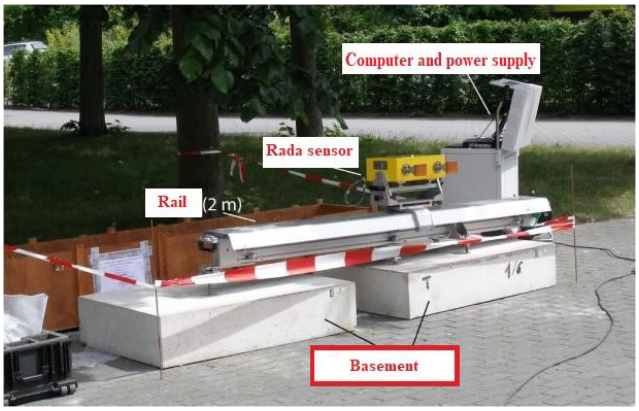


**FIGURE 1.** Ground-based radar system.

from GB-SAR dataset with high precision which also can be proved by the consistence with the pendulums monitoring results. Compared with traditional sensors, the proposed monitoring technique has advantages of non-contact and visual measurement that can be employed widely in the field displacement measurement of different objects, including bridges, slopes and glaciers [6].

## II. GBINSAR PRINCIPLES

Ground-based InSAR technology can obtain 2D images illuminating the monitoring area through its active microwave detection capability. The high spatial resolution in both azimuth and range can be improved by the synthetic aperture and stepped frequency techniques. Severe temporal–spatial decoherence and low resolution of satellite SAR images can be prevented by ground-based interferometry technology. Displacement less than one millimetre can be detected by this precise and accurate approach.

GBInSAR technology can monitor tiny displacements along the radar LOS accurately. Two-dimensional images of the monitoring area obtained by the ground radar have high range resolution improved by the SF-CW technology and nice azimuth resolution enhanced by the synthetic aperture technique. Finally, the deformation can be extracted by interference technique for the monitoring area [7].

Image by interferometric survey (IBIS) is a ground-based microwave interferometer system that possesses the imaging capability to remotely monitor long-distance targets which was invented by IDL company and University of Florence [8]. The IBIS-L shown in the Fig. 1 is an innovative radar based on microwave interference technology, which has detecting distance of up to 4 km and an accuracy of 0.1 mm. Compared with GPS, total station and other instruments, IBIS-L has the advantage of continuous coverage and remote monitoring ability. IBIS-L plays an important role in the deformation laws analysis and accidents prevention. This precise instrument owns three main advanced technologies, i.e. SF-CW, SAR and interferometry. The following text is a brief description of the SF-CW and synthetic aperture technologies [8].

### A. SF-CW ECHNOLOGY

A radar system can produce a group of electromagnetic waves with different frequencies through the SF-CW technology to guarantee the long-distance transmission of electromagnetic waves during sweep time. Thanks to the technique above, the resolution in the range direction can be improved for ground radar. The frequency bandwidth is $3 \times 10^8$; range resolution is calculated using the formula $\Delta$ r = C/2B is 0.5 m. This formula means that each 0.5 m of monitoring area is divided into one unit along the radial direction [9].

### B. SYNTHETIC APERTURE TECHNOLOGY

Basically, Synthetic aperture technology is a Doppler analysis technology. The small Doppler shift difference between different azimuth scatters in the same range unit can be detected by radar motion to generate better azimuth resolution. In brief, the real antenna with small size can be simulated as a long one by radar motion, which is called 'synthetic aperture' [10].

## III. MATERIALS AND METHODS

### A. METHODS OF DEFORMATION RATE EXTRACTION BASED ON PS FOR DAM

The GB-SAR technology can perform high-precision measurements on different targets, such as dams and bridges [11]–[13], but different target objects have the different technical characteristics. Thus, a meticulous monitoring program should be designed that combines their characteristics. The IBIS-L was employed to monitor Geheyan Dam and simultaneously the linear deformation of the dam surface was extracted by this technology. The feasibility of this deformation monitoring technology is proven in this study. The process flow of the time-series analysis based on PS theory for Geheyan Dam presented in this section is shown in Fig. 2.

### B. MEASUREMENT CAMPAIGN IN THE GEHEYAN DAM

The Geheyan hydropower station is built on the mainstream of the Qingjiang River in Changyang County, Hubei Province, China. The Geheyan Dam is a double-track gravity arch dam with a crest elevation of 206 m, a crest length of 665.45 m and dam height of 151 m. The gravity dam sections are arranged on both banks (see Fig. 3), and gravity piers are installed on the base surface of the left bank with elevations of 120 m to 138 m. The dam is 207 km away from Enshi City and 50 km away from the Gaobazhou Hydropower Station. The power generation system combines flood control and shipping functions. The hub project mainly consists of a gravity arch dam, a discharge building, a water diversion type hydropower station on the right bank, and a vertical ship lift on the left.

Fig. 4 shows that the discharge building is mainly arranged in the middle of the dam bed. The overflow leading edge is 188 m in length with seven overflowing orifices, four deep holes and two bottom outlets. The overflow crest elevation is 181.8 m and the orifice size are 12 m $\times$ 18.2 m.

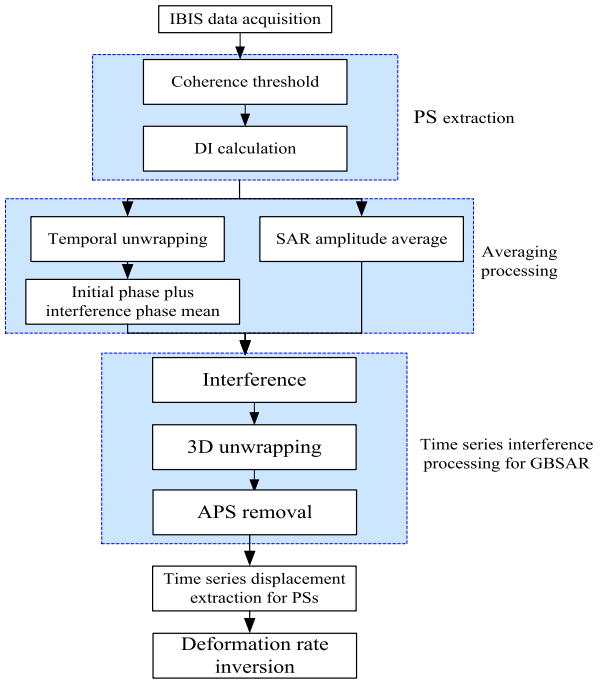


**FIGURE 2.** GB-InSAR process for dam monitoring.

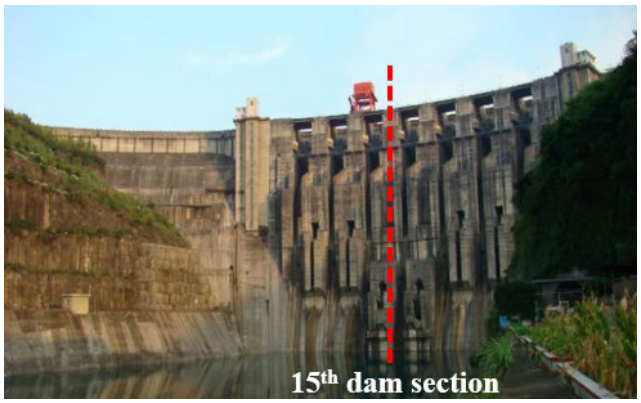


**FIGURE 3.** Close shot of Geheyan Dam and plumb line layout.

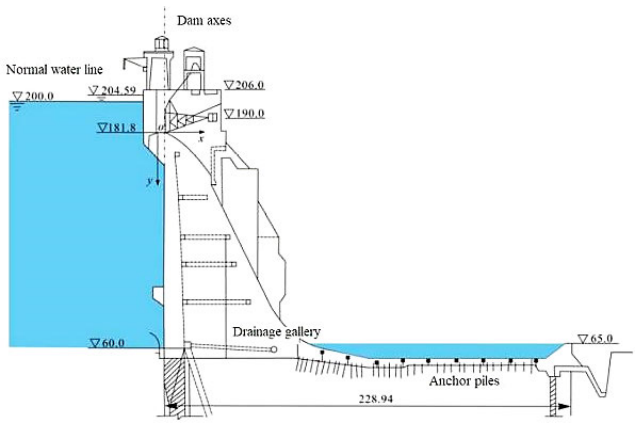


**FIGURE 4.** Structure of Geheyan Dam.

The bottom of the deep hole elevation is 134 m and their size are 4.5 m × 6.5 m. The height of the bottom hole is 95 m, and the orifice size is 4.5 m × 6.5 m. All orifices are controlled by arc gates, and flat-panel maintenance gates are installed in the upstream.

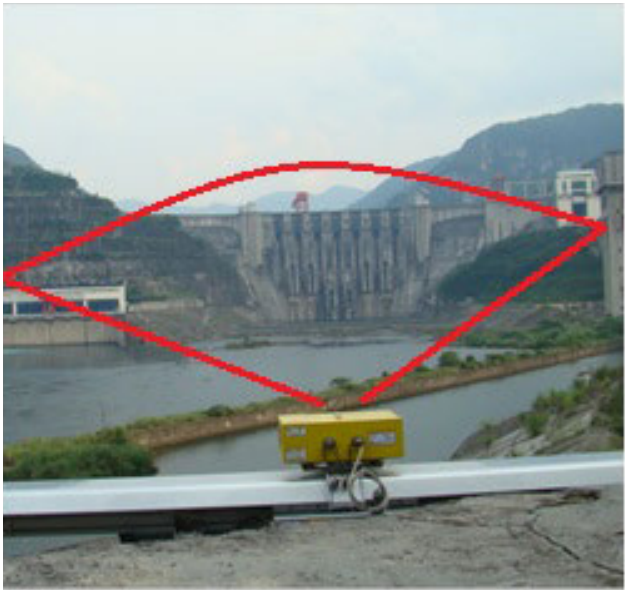

**FIGURE 5.** Location and illumination field of radar.

**TABLE 1.** Radar equipment parameters.

| Symbol | Value |
|---|---|
| Rail Length | 2m |
| Center Frequency | 16.75GHz |
| Max Range | 1.3km |
| Polarization | VV |
| Brand Width | 300MHz |
| Range Resolution | 0.5m |
| Azimuth Resolution | 4.4mrad |
| Elevation Angle | 0° |

This experiment mainly monitors the dam for a long time without interruptions. The radar equipment is installed on the left bank in the downstream at approximately 1 km away from the dam. The guide rail is arranged in a horizontal plane. The centre line of radar is positioned towards the right side of the dam body, and the main body and the right bank side of this dam are within the illuminated field of the radar, as shown in Fig. 5. The IBIS performed continuous monitoring from 8:24 AM on July 27, 2015 and to 11:08 on August 2, 2015. A total of 1,330 ground-based SAR images were collected. The main parameters of the radar equipment are listed in TABLE 1. Several interruptions occurred during the monitoring procedure due to heavy rainfall, thunder and other bad weather conditions. Detailed information on the interruptions can be found in TABLE 2.

**TABLE 2.** Data collection with interruptions.

| Number | Interruption time | Reason | Interruption duration |
|---|---|---|---|
| 1 | 2015.07.29 - 20:33 | Thundershower | 2h59min |
| 2 | 2015.07.30 - 10:19 | Breakdown | 1h1min |
| 3 | 2015.08.01 - 04:17. | Breakdown | 2h51min |
| 4 | 2015.08.01 - 23:21 | Thundershower | 7h10min |

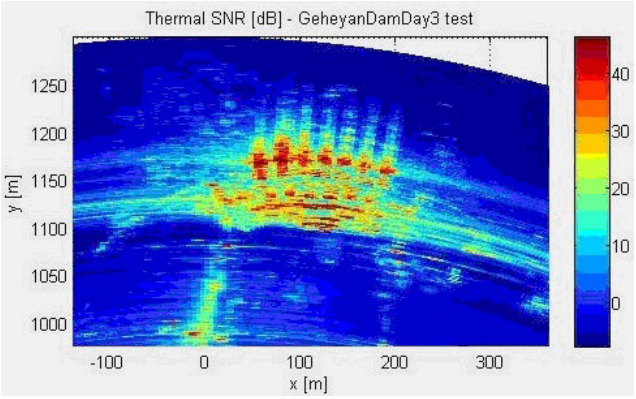


**FIGURE 6.** Thermal signal-to-noise ratio of dam.

Geheyan Dam is completely made of concrete and covered by few vegetation near the mountain the dam has a strong thermal signal-to-noise ratio (TSNR) under radar illumination. the scattering signals of the dam body can be proved very high during the monitoring period in Fig. 6. The average TSNR value exceeds 25 dB, and some scattering signals are greater than 40 dB. The dam structure can be discerned from the TSNR map so clearly including the 7 orifice gates. Furthermore, the reflected signals of these gates collected by GB-SAR are stronger than the other parts of the dam because they are made of metal. However, these gates were imaged with different spatial signature of them due to the long monitoring distance between the radar centre and dam. The qualified dataset with high TSNR can be guaranteed for the long-term continuous monitoring by ground-based SAR [14].

### C. ATMOSPHERIC PHASE CORRECTION BASED ON PS ANALYSIS

For GBSAR measurement, the signals received by the radar sensor always are affected by the serious atmospheric turbulence. The refractive index $n$ described by a function of absolute temperature $T$, air pressure $P$ and humidity $H$ can be employed as a simple model explaining their physical

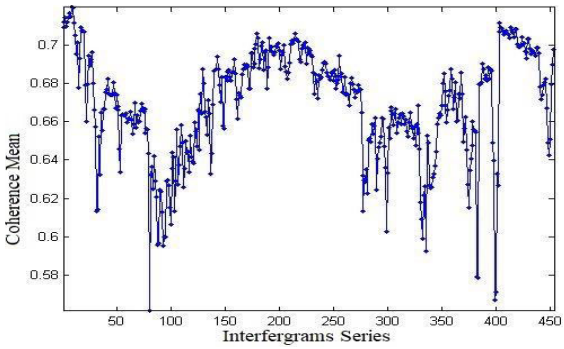


**FIGURE 7.** Remove the temporal coherence mean of low-quality images.

existence [15]. Usually, the refractive index $n$ is very close to 1. For the convenience of calculation and analysis, the refraction degree N is used to represent the radio propagation, that is

$$\mathrm{N} = (n-1) \times 10^6 \tag{1}$$

Tropospheric delay can be divided into dry delay component $\mathrm{N}_{dry}$ and wet delay component $\mathrm{N}_{wet}$. According to the empirical model of atmospheric refraction, the refraction degree N can be expressed by the formula (2):

$$\begin{aligned} \mathrm{N} &= \mathrm{N}(P,T,H) = \mathrm{N}_{dry} + \mathrm{N}_{wet} \\ &= 0.2589\frac{P_d}{T} + (71.7 + \frac{3.744 \times 10^5}{T})\frac{e}{T} \end{aligned} \tag{2}$$

Among them, $P$ is the total atmospheric pressure, dry gas pressure is $P_d$, water vapor pressure is $e$, the both units are mbar, and the relationship between them was $P_d = P - e$.

Moreover, the plumb line measurement of the dam started from 8:00 am on the 30st July, 457 scenes of GBSAR images were collected at the same time to accomplish the deformation analysis of the dam and the measurement results verification. During the monitoring period, several monitoring interruptions occurred due to bad weather conditions or special problems caused by the IBIS itself. Therefore, we should determine whether or not low-quality SAR images are affected by this issue. Images with a coherence threshold of 0.56 are selected in the time series, and three images with poor coherence are excluded from the experiment [13]. Finally, the overall higher coherent mean value is shown in Fig. 7.

Fig. 8 shows the coherence mean histogram for each pixel in all selected images. The temporal coherence indicates that the pixels are larger than 0.55, and the coherence indicates that the pixels that represent the dam body are near 0.9. Two thresholds are used in this study to extract the PS points. Considering the data quality and the distribution of the points, we use a 5 × 5 window to calculate the coherence and choose 0.8 as the coherence threshold and 0.3 as the amplitude dispersion index threshold. The PS extraction results are shown in Fig. 9. The dual thresholds method can remove the points with false signals and leave the points with high

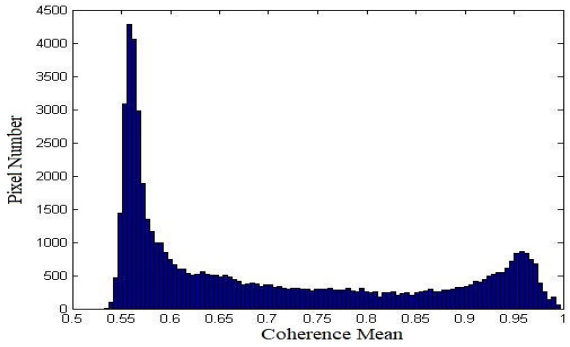


**FIGURE 8.** Coherent histogram of all pixels of the image.

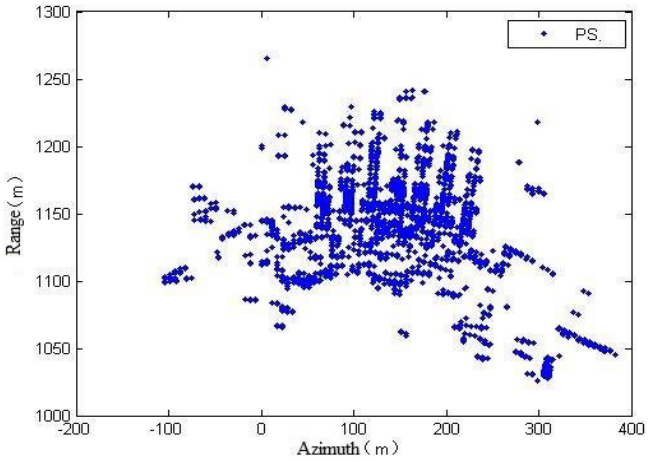


**FIGURE 9.** Dual threshold extraction of PS points.

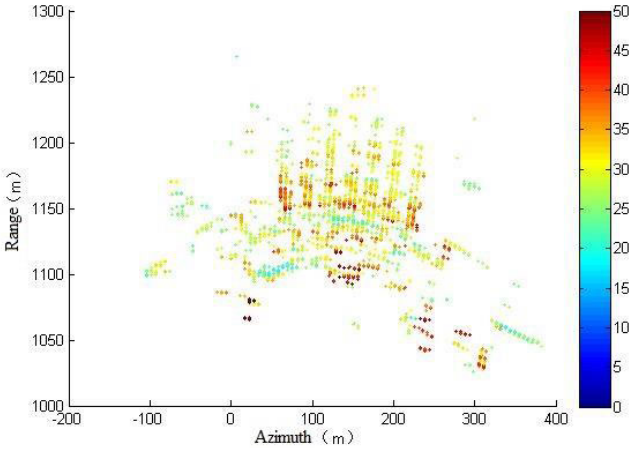


**FIGURE 10.** Signal noise ratio (SNR) of PS points (dB).

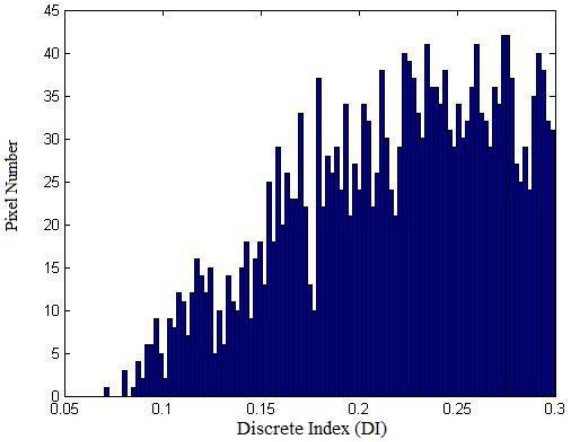


**FIGURE 11.** PS point DI histogram.

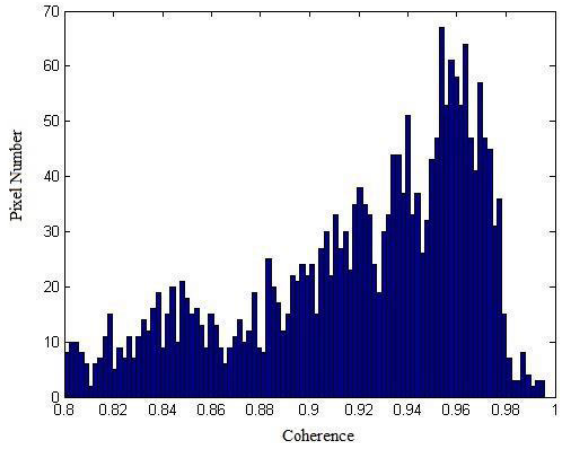


**FIGURE 12.** PS Point coherence histogram.

spatial–temporal coherence. The SNRs of the extracted PS points exceed 25 dB, and the points of each dam section are mostly extracted (Fig. 10). Discrete index (DI) [6] and the coherence histograms of the PS points are shown in Figs. 11 and 12, respectively. Most of the PS points in the DI histogram are around 0.2, and the coherent means of these points are mainly within [0.9, 1]. A total of 2,733 PS points was calculated, which is approximately 5% of the total number of pixels. The points are mainly distributed rationally on both sides of the dam and abutment.

The amount of data is large and weather conditions change drastically because the monitoring period spans three days. Before the time-series interference processing, temporal 'multi-look processing' for time-series SAR images is implemented in this study to improve operating efficiency and reduce the phase noise because the research scene does not change significantly within a short time interval. Thus, the average of five neighbouring images is calculated in continuous observations, which can reduce the impact of the random noise mixed in the phases and improve calculation efficiency [16].

GB-SAR monitoring data has a long-time span and dramatic meteorological changes. PS phases in the stable region are used to fit the atmospheric phase to each interference image. The fitted atmospheric phase values of the PS points at different collection times on July 31 are shown in Fig. 13, especially at noon when the atmospheric phase values are large.

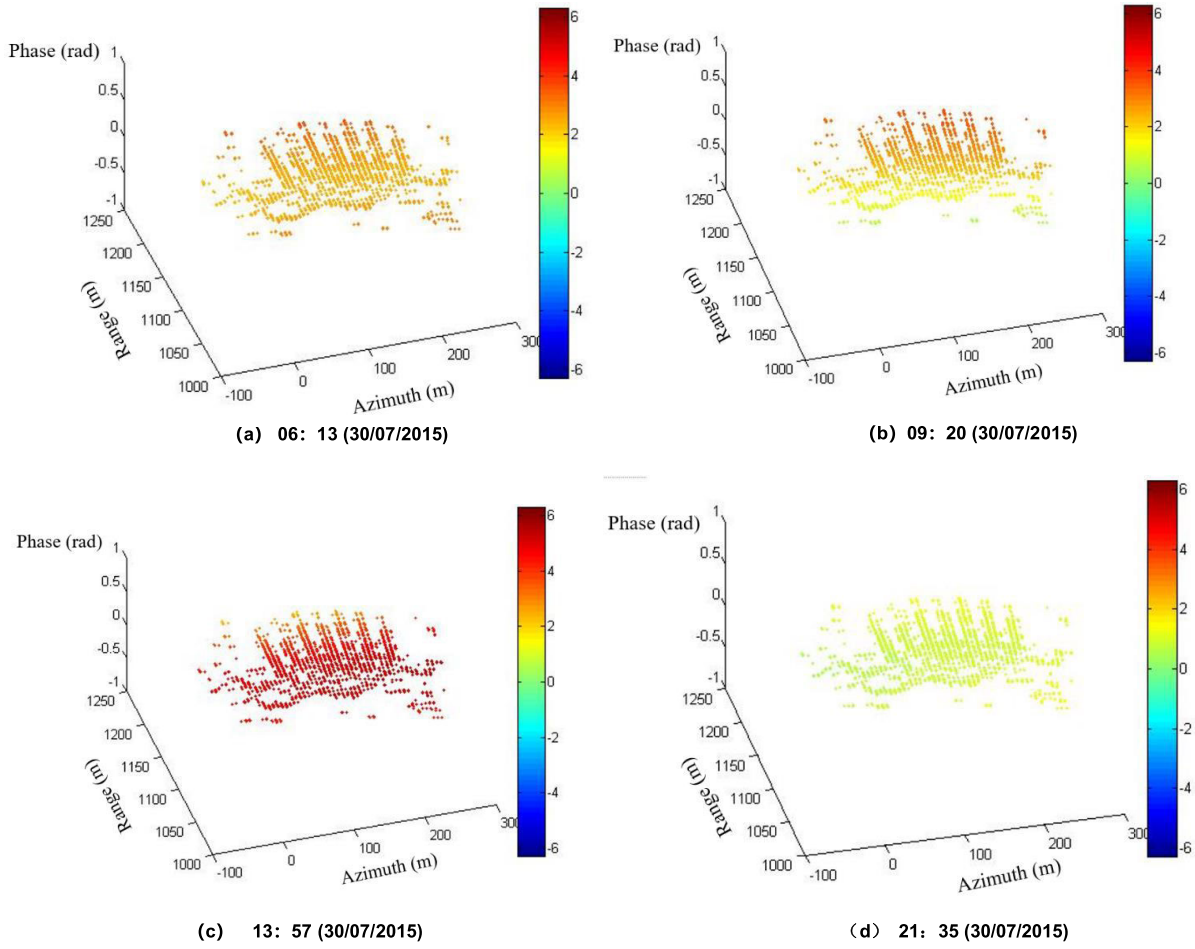


**FIGURE 13.** Atmospheric phase diagrams at PS points at different observed times (rad).

The stable areas can be recognized by the priori knowledge which can be employed for the turbulence atmosphere extraction, the detailed procedure of atmosphere phase screen correction is described in [17]. Therefore, the deformation information on the dam surface can be obtained after the atmospheric phase is removed. To analyse the spatial deformation characteristics of the dam, the surface deformation is investigated by selecting the PS displacement results acquired at different times, as shown in Fig. 14. During the entire observation period, the performance of dam surface was relatively stable since 8:06 of the 31$^{st}$. The entire dam deformation was within 0.5 mm, and a displacement of more than 0.5 mm occurred in the upper middle of the dam at 21:38 that day but the other dam sections were relatively stable. The deformation of the upper part of the dam gradually increased from 00:41 on 1$^{st}$ Aug, and the displacements of some PS points were close to 2 mm. At 20:48, the dam's body had a deformation of nearly 2 mm. The deformation tendency gradually weakened by 7:05 on the second. In the vertical direction of the dam, the deformation trend gradually decreased from the top to the bottom. Afterwards, the overall stability of the dam was relatively stable since 8:47, although a few PS points were greatly affected by the turbulence noise.

## IV. RESULTS

The plumb monitoring measurement for Geheyan Dam has been performed during the same period. Due to different reference point selected between the plumb lines and GB-SAR results, these two sequential displacements never be compared with each other directly. However, the deformation ratio extracted from radial deflection displacement of dam body can reflect the different trends for dam structure during the monitoring period. Obvious linear trends for most part of dam can be found from the fitted ratio results shown in Fig.15. Considering the difficulty in deformation analysis caused by the large amount of data, all measured data are fitted linearly according to the acquisition time to obtain the deformation rate of different PS points during the monitoring period.

For better comparation with pendulum measurements data, the digital surface model of Geheyan Dam has been obtained by 3D laser scanning sensor before the GB-SAR measurement campaign. Therefore, the GB-SAR data can be geocoded by using this fusion method of GB-SAR and 3D scanning data which is not main propose of this article. The entire fusion procedure is fully detailed in the article [18], and the fusion image of these two sensors is shown in the Fig.16. To compare the GBSAR result with the plumb line

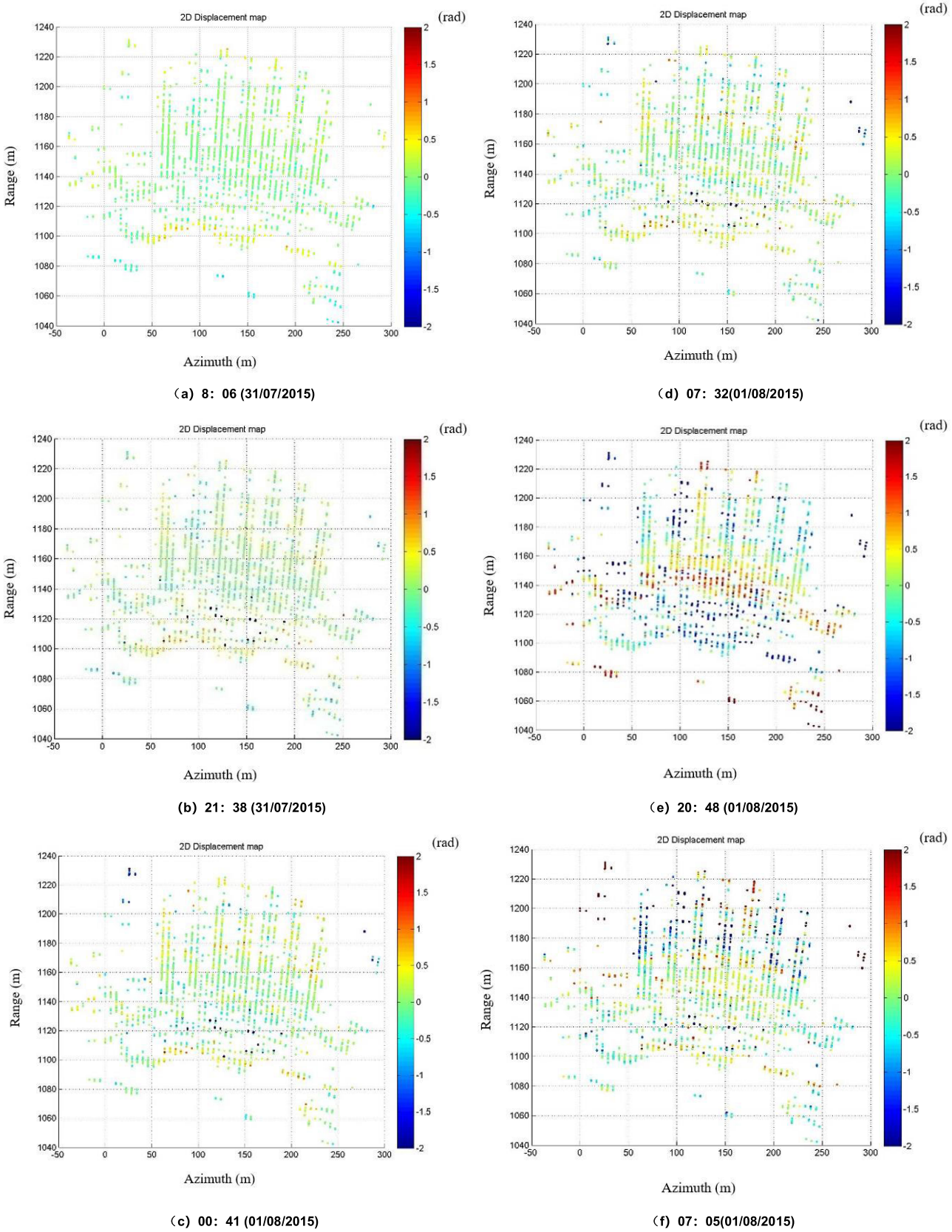


**FIGURE 14.** Observational deformation diagram of PS points on dam during the observation period.

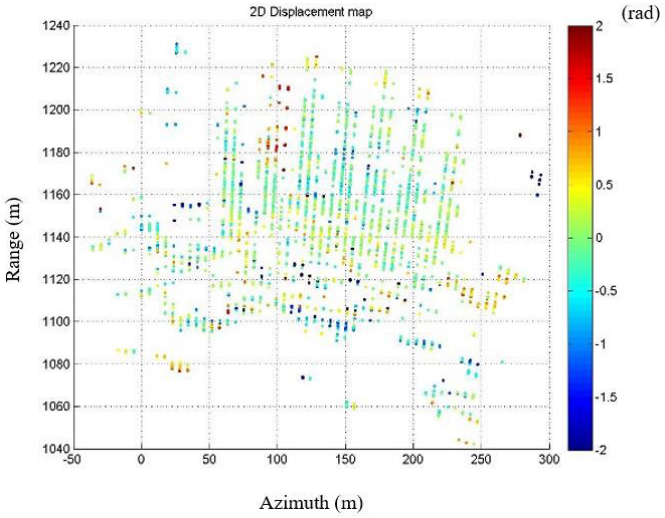


(g) 08: 47 (02/08/2015)

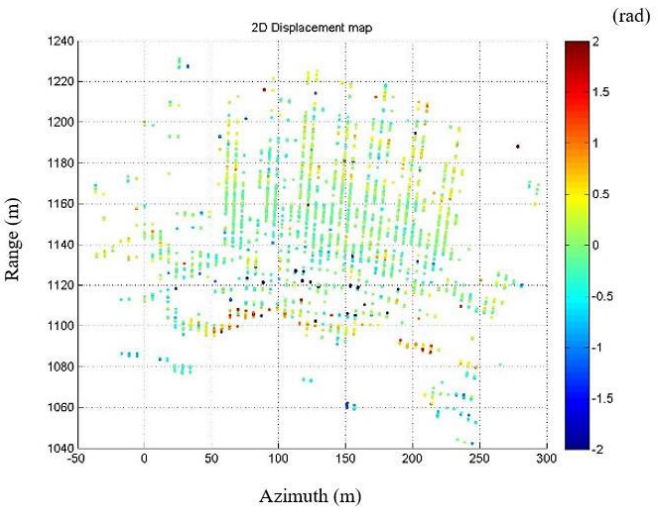


(h) 11: 02 (02/08/2015)

**FIGURE 14.** *(Continued.)* **Observational deformation diagram of PS points on dam during the observation period.**

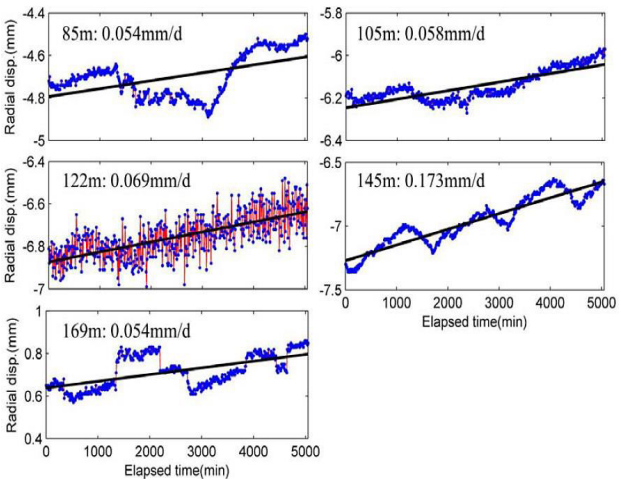


**FIGURE 15.** **Linear fitting results of the plumb monitoring data.**

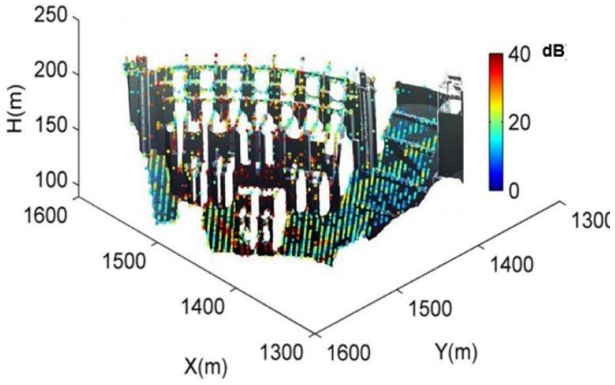


**FIGURE 16.** **Fusion image of 3D scanning points and TSNR of the dam.**

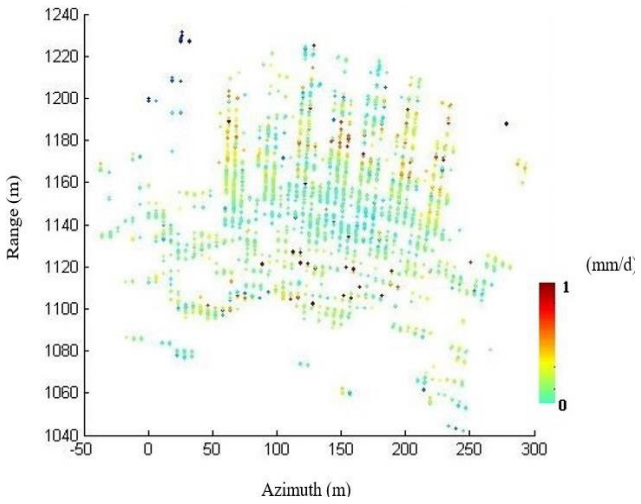


**FIGURE 17.** **The deformation rate map of the dam surface.**

result, linear regression analysis is used to linearly fit the dam surface deformation trend to the monitoring time sequence. The deformation rate inversion results of the entire dam surface are obtained, as shown in Fig. 17. The deformation of the dam presents a layer distribution, the deformation at the upper middle of the dam is the largest and those at the bottom and top are small. The average calculated by the radium of 3 pixels selected from the PS points on the 15th dam section is taken as the base point in this study.

Furthermore, the linear rate extracted from the GBSAR data of the entire dam and that obtained from plumb line monitoring are compared [19], [20]. Combined with the fusion results, the pendulums results of the 15th dam section marked with red dotted line in Fig.3 are 0.054, 0.058, 0.069, 0.173, and 0.054 mm/d, which correspond to the different heights of the dam from the bottom to the top (TABLE 3).

TABLE 3 shows that the dam surface deformation monitoring results obtained in this study are basically consistent with the observed plumb lines, but those at the dam heights

**TABLE 3. Comparison of deformation rate extraction with plumb line method.**

| Dam Elevation | Plumb Results(mm/d) | Proposed Results(mm/d) |
|---|---|---|
| 169 | 0.054 | 0.066 |
| 145 | 0.173 | 0.256 |
| 122 | 0.069 | 0.142 |
| 105 | 0.058 | 0.103 |
| 85 | 0.054 | 0.0341 |

of 122 m and 105 m are slightly different from those of the plumb lines [21]. This finding may be caused by the incomplete removal of atmospheric noise. The averaging method of base point extraction is employed to obtain the corresponding monitoring results, which may include some PS points with poor quality. Therefore, the results may suffer with uncertain deviations. According to the results monitored by this GB-SAR campaign, obviously we can find that the deformation of the dam spillway gates is greater than that of the dam body, and with the increase of the water level in the reservoir area, the displacement increases along the direction of water flow gradually. Moreover, the basement of Geheyan Dam is very stable compared with the other parts because the deformation rate with hight 85m is less than 0.06mm/d. A generally better monitoring approach is proposed in this study based on the GB-SAR long-term monitoring data. The approach can extract the deformation trend of the dam surface accurately and provide important decision guidance for the safety monitoring and management of large-scale projects.

## V. CONCLUSION

This work focuses on the deformation monitoring method for dams using GBSAR data. Sequential GB-SAR data is analysed and the deformation results are extracted from temporal displacements based on PS points to monitor Geheyan Dam in this article. Some important conclusions can be listed as below:

(1). GB-SAR equipment can illuminate the monitoring areas with regional scale and obtain time series displacement for 2 dimensions (range and azimuth), which is more powerful than traditional single-point monitoring information.

(2). The atmosphere effects are increasing with the distance between the radar centre and monitoring objects. The time series deformation extraction can be accomplished only after atmospheric phase screen reduction, especially for the dam measurement campaign due to the violent changes of temperature and humidity during the monitoring period.

(3). The surface deformation rate of the dam body is investigated by linear regression analysis, and the inversion results are compared and verified with the plumb line results. The structure of Geheyan Dam is stable during the monitoring period based on GB-SAR monitoring results, which is analysed by the time series technology in this study [6].

## AUTHOR CONTRIBUTIONS

**Z.Q.** carried out the preliminary studies, participated in the drafted the manuscript. **M.J.** participated in the design of the study and performed the statistical analysis. **T.J.** conceived of the study, and **L.Z.** participated in its design and coordinatio and helped to draft the manuscript. All authors read and approved the final manuscript.

## ADDITIONAL INFORMATION

Competing Interests: The authors declare no competing interests.

## COMPUTER CODE AVAILABILITY

The source code, example input data, and user manul are available at https://github.com/ZhiweiQiu/GBSARforDam

## REFERENCES


[1] D. Hölbling, P. Füreder, F. Antolini, F. Cigna, N. Casagli, and S. Lang, "A semi-automated object-based approach for landslide detection validated by persistent scatterer interferometry measures and landslide inventories," *Remote Sens.*, vol. 4, no. 5, pp. 1310–1336, May 2012.

[2] F. Bozzano, I. Cipriani, P. Mazzanti, and A. Prestininzi, "Displacement patterns of a landslide affected by human activities: Insights from ground-based InSAR monitoring," *Natural Hazards*, vol. 59, no. 3, pp. 1377–1396, Dec. 2011.

[3] D. Giordan, P. Allasia, N. Dematteis, F. Dell'Anese, M. Vagliasindi, and E. Motta, "A low-cost optical remote sensing application for glacier deformation monitoring in an alpine environment," *Sensors*, vol. 16, no. 10, p. 1750, Oct. 2016.

[4] T. Wang and S. I. Jonsson, "Improved SAR amplitude image offset measurements for deriving three-dimensional coseismic displacements," *IEEE J. Sel. Topics Appl. Earth Observ. Remote Sens.*, vol. 8, no. 7, pp. 3271–3278, Feb. 2015.

[5] A. Ferretti, C. Prati, and F. Rocca, "Permanent scatterers in SAR interferometry," *IEEE Trans. Geosci. Remote Sens.*, vol. 39, no. 1, pp. 8–20, Jan. 2001.

[6] D. Dei, M. Pieraccini, M. Fratini, C. Atzeni, and G. Bartoli, "Detection of vertical bending and torsional movements of a bridge using a coherent radar," *NDT E Int.*, vol. 42, no. 8, pp. 741–747, Dec. 2009.

[7] L. C. Graham, "Synthetic interferometer radar for topographic mapping," *Proc. IEEE*, vol. 62, no. 6, pp. 763–768, Jun. 1974.

[8] G. Herrera, J. A. Fernández-Merodo, J. Mulas, M. Pastor, G. Luzi, and O. Monserrat, "A landslide forecasting model using ground based SAR data: The portalet case study," *Eng. Geol.*, vol. 105, nos. 3–4, pp. 220–230, May 2009.

[9] S. A. Hovanessian, *Introduction to Synthetic Array and Imaging Radars*. Dedham, MA, USA: Artech House, 1980.

[10] Y. Jianping, F. Lu, and L. Ni, "Research advances of theory and technology in deformation monitoring," *Bull Surv. Map*, vol. 7, pp. 1–4, Jan. 2007.

[11] H. Lee, J.-H. Lee, S.-J. Cho, N.-H. Sung, and J.-H. Kim, "An experiment of GB-SAR interperometric measurement of target displacement and atmospheric correction," in *Proc. IEEE Int. Geosci. Remote Sens. Symp. (IGARSS)*, Kuala Lumpur, Malaysia, Jun. 2008, pp. 240–243.

[12] F. Bardi, W. Frodella, A. Ciampalini, S. Bianchini, C. Del Ventisette, G. Gigli, R. Fanti, S. Moretti, G. Basile, and N. Casagli, "Integration between ground based and satellite SAR data in landslide mapping: The San Fratello case study," *Geomorphology*, vol. 223, pp. 45–60, Oct. 2014.

[13] M. Alba, G. Bernardini, A. Giussani, P. P. Ricci, F. Roncoroni, M. Scaioni, P. Valgoi, and K. Zhang, "Measurement of dam deformations by terrestrial interferometric techniques," in *Proc. Congr. Int. Soc. Photogramm. Remote Sens. (ISPRS).*, Beijing, China, 2008, pp. 133–139.

[14] L. Mascolo, G. Nico, and A. Pitullo, "Merging ground-based and spaceborne InSAR data to monitor an earth dam," in *Proc. Fringe, Adv. Sci. Appl. SAR Interferometry Sentinel-1 InSAR Workshop*, May 2015, p. 19.

[15] J. Yue, Z. Qiu, X. Wang, and S. Yue, "Atmospheric phase correction using permanent scatterers in ground-based radar interferometry," *J. Appl. Remote Sens.*, vol. 10, no. 4, Nov. 2016, Art. no. 046013, doi: 10.1117/1.JRS.10.046013.

[16] L. Pipia, X. Fabregas, A. Aguasca, C. Lopez-Martinez, J. Mallorqui, and O. Mora, "A subsidence monitoring project using a polarimetric GB-SAR sensor," in *Proc. Workshop POLinSAR*, no. 1, 2007, pp. 22–26.
[17] Z. Qiu, Y. Ma, and X. Guo, "Atmospheric phase screen correction in ground-based SAR with PS technique," *SpringerPlus*, vol. 5, no. 1, p. 1594, Dec. 2016.
[18] J. Zou, J. Tian, Y. M. Q. Chen, and Q. Li, "Research on data fusion method of ground-based SAR and 3D laser scanning," *J. Geomatics*, vol. 40, pp. 26–30, Jun. 2015, doi: 10.14188/j.2095-6045.
[19] K. Takahashi, M. Matsumoto, and M. Sato, "Continuous observation of natural-disaster-affected areas using ground-based SAR interferometry," *IEEE J. Sel. Topics Appl. Earth Observ. Remote Sens.*, vol. 6, no. 3, pp. 1286–1294, Jun. 2013.
[20] G. Bernardini, N. Gallino, C. Gentile, and P. Ricci, "Dynamic monitoring of civil engineering structures by microwave interferometer," in *Proc. Conceptual Approach Struct. Design*, Venice, Italy, no. 6, 2007, pp. 1–10.
[21] S. Gamse, M. J. Henriques, and M. Oberguggenberger, "Assessment of long-term pendulum and geodetic observations on a concrete arch dam," in *Proc. 3rd Joint Int. Symp. Deformation Monitoring*, 2016, pp. 1–8.

**ZHIWEI QIU** received the master's degree in photogrammetry and remote sensing from Wuhan University, Wuhan, China, in 2009, and the Ph.D. degree in geophysics and geodesy from Hohai University, Nanjing, China.

From 2010 to 2016, he was a Research Assistant with the Henan University of Urban Construction, Pingdingshan, Henan, China. He is currently a Teacher with Jiangsu Ocean University, Lianyungang, China. He specializes in SAR data processing and deformation monitoring. His research interests include the development of remote sensing and InSAR techniques using time series analysis, fundamental study of photogrammetry, and application of ocean remote sensing.

**MINGLIAN JIAO** received the bachelor's degree in surveying engineering from Henan Polytechnic University, Jiaozuo, China. He is currently a Professor with the School of Surveying and Ocean Information, Jiangsu Ocean University. He specializes in surveying engineering and mapping.

**TINCHEN JIANG** received the Ph.D. degree in surveying engineering from Wuhan University, Wuhan, China. He is currently a Professor with the School of Surveying and Ocean Information, Jiangsu Ocean University. His research interests include interferometric synthetic aperture radar for inverting source parameters of earthquakes and ground deformation monitoring in urban areas.

**LI ZHOU** received the master's degree from the China University of Mining and Technology. He is currently a Professor with the School of Surveying and Ocean Information, Jiangsu Ocean University. His current research interests include the ocean remote sensing application and spatial-temporal analysis.